Nanoporous Silica Prepared with Activated Carbon Molds Using Supercritical CO_2

H. Wakayama* and Y. Fukushima

Toyota Central R&D Labs., Inc., Nagakute, Aichi, 480-1192, Japan

Received August 2, 1999

Nanoporous silica materials have been prepared using an activated carbon as a mold and supercritical carbon dioxide as a solvent. Tetraethyl orthosilicate (TEOS) dissolved in supercritical carbon dioxide was in contact with the activated carbon templates of various macroscopic shapes (fibers, granules, powders). After the removal of activated carbon templates by calcination in air or oxygen plasma treatment, microporous and mesoporous silica samples replicating not only mesostructures, but also macroscopic shapes, of activated carbon molds were obtained. The pore size of the silica replicas increases with increase in carbon crystallite size of activated carbon as estimated from XRD patterns.

Introduction

Porous materials are very attractive because of the physicochemical properties of porous structures and surface characters. These materials have found application in adsorbates, catalysts, and capacitors. Microporous and mesoporous materials have excellent potential for applications in highly selective adsorbates, because it would be expected that micropores adsorb some molecules with high selectivity and mesopores facilitate mass transfer. Macroscopic shapes of porous materials are also important for applications. Many studies have been performed on controlling their structures with the use of templates.[1−5] Material synthesis using molds is also important in industrial processes such as plastic molding[6] or metal casting. In these processes, coating raw materials uniformly on the mold surface or filling raw materials into the spaces in molds is very important for precise replication of the structures of the molds.

Supercritical fluids are of great focused because of their unique properties.[7] They have low viscosity and high diffusivity.[8] The solubility can be controlled by changing the temperature and pressure or by adding a modifier.[9] Thus, supercritical fluids are expected to carry an effective quantity of raw materials' precursors into the fine spaces. Especially important is that supercritical carbon dioxide can be handled easily because it is nonflammable, nontoxic, inexpensive, and has low critical temperature. On the other hand, supercritical carbon dioxide is a nonpolar solvent and can barely dissolve polar materials such as most of inorganics. Most researchers use supercritical alcohol[10] or water[11] in the synthesis of inorganic materials as supercritical solvents.

We have proposed a novel process for material synthesis called "nanoscale casting using supercritical fluids (NC-SCF)"[12−14] in which precursors of the raw materials are dissolved in supercritical CO_2 and are attached to activated carbon molds. After the activated carbon are removed from the samples coated with Pt or other materials, porous materials replicating not only macroscopic shapes (e.g., fibrous) but also porous structures in nanometer scale can be obtained. This process can be applied to the synthesis of not only metals (e.g., Pt)[12] but oxide (e.g., silica).[13−14] However, detailed studies are necessary to confirm the micro- to mesoscale replications.

Here, we studied the influences of templates on the porous structures of silica cast-off skins by using several kinds of activated carbon to demonstrate the mesoscale replication.

Experimental Section

Chemicals. Tetraethyl orthosilicate (TEOS, Wako Pure Chemical Industries, Ltd.) was used as silica source. Solid carbon dioxide (dry ice) was obtained from Marukyo Oxygen Company. Activated carbon fibers A-20 and activated carbon powders M30 were obtained from Osaka Gas Chemical Company; activated carbon fibers BW103, from Toyobo Co., Ltd.;

* E-mail: wakayama@mosk.tytlabs.co.jp.

(1) Meier, W. N.; Olson, D. H. *Atlas of Zeolite Structure Types*, 2nd ed.; Butterworths: London, 1988.
(2) Satishkumar, B. C.; Govindaraj, A.; Vogl, E. M.; Basumallick, Lipika; Rao, C. N. R. *J. Mater. Res.* **1997**, *12*, 604.
(3) Kresge, C. T.; Leonowicz, M. E.; Roth, W. J.; Vartuli, J. C.; Beck, J. S. *Nature* **1992**, *359*, 710.
(4) Velev, O. D.; Jede, T. A.; Loba, R. F.; Lenhoff, A. M. *Nature* **1997**, *389*, 447.
(5) Templin, M.; Franck, A.; Chsne, A. D.; Leist, H.; Zhang, Y.; Ulrich, R.; Schandler, V.; Wiesner, U. *Science* **1997**, *278*, 1795.
(6) Rubin, I. I. *Injection Molding Theory and Practice*; Wiley: New York, 1972.
(7) Darr, J. A.; Poliakoff, M. *Chem. Rev.* **1999**, *99*, 495.
(8) Etesse, P.; Zega, J. A.; Kobayashi, R. *J. Chem. Phys.* **1992**, *97*, 2022.
(9) Dobbs, J. M.; Wong, J. M.; Lahiere, R. J.; Johnston, K. P. *Ind. Eng. Chem. Res.* **1987**, *26*, 56.
(10) Chhor, K.; Bocquet, J. F.; Pommier, C. *Mater. Chem. Phys.* **1992**, *70*, 73.
(11) Matson, D. W.; Fulton, J. L.; Petersen, R. C.; Smith, R. D. *Ind. Eng. Chem. Res.* **1987**, *26*, 2298.
(12) Wakayama, H.; Fukushima, Y. *Chem. Commun.* **1999**, *4*, 391.
(13) Wakayama, H.; Fukushima, Y. Proceedings of 6th Meeting on Supercritical Fluids, Nottingham, UK, 1999; p 721.
(14) Fukushima, Y.; Wakayama, H. *J. Phys. Chem. B* **1999**, *103*, 3062.

10.1021/cm990487e CCC: $19.00
Published on Web 03/02/2000

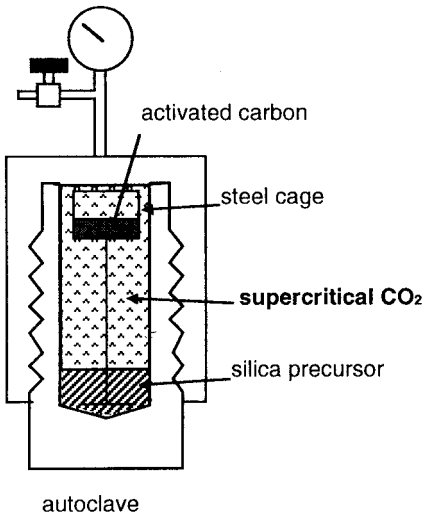

Figure 1. Schematic illustration of an autoclave and a cage used to treat samples in supercritical carbon dioxide.

activated carbon granules and D7, from Kurare Chemical Company; and activated carbon from palm nutshell (GC-2), from Takeda Chemical Industries Ltd.

Synthesis in Supercritical Carbon Dioxide. Tetraethyl orthosilicate(3 mL) was placed in a stainless steel autoclave of 50-mL capacity. A total of 1 g of activated carbon was placed in a stainless cage fixed at the upper part of the autoclave without touching with liquid TEOS at the bottom, as shown in Figure 1. Carbon dioxide then filled in the autoclave. The autoclave was heated at 393 K for 2 h in an oil bath, and the inside pressure was 26 MPa under a typical condition. After cooling to room temperature, samples were heated at 378 K for 12 h in normal atmospheres.

Synthesis in Liquid Silica Precursor (TEOS). For the comparison, samples were prepared without using supercritical fluids, in which activated carbon was immersed in 30 mL of liquid TEOS. The samples were heated at 393 K for 2 h, followed by drying at 378 K for 12 h.

Calcination Procedure. The activated carbon was removed by calcination at 873 K for 6 h in air flow. As an alternative way to remove activated carbon, samples were treated in oxygen plasma at 500 W in oxygen flow (160 mL/min) using a YAMATO Scientific oxygen plasma equipment (PC-103, RFG-500).

Analyses. Nitrogen adsorption−desorption isotherms were obtained at 77 K on a QUANTACROME AUTOSORP-1-MP. Before this measurement, samples were heated at 423 K in 10^{-6} Torr for 3 h. Density functional theory (DFT) and the Barret−Joyner−Hallender (BJH) method on desorption branch were used to determine the pore size distributions for pore diameters up to 2 nm and for those above 2 nm in diameter, respectively. X-ray diffraction data for activated carbon was recorded by RIGAKU RINT-2000 using Cu Kα radiation and 2°(2θ)/min of scanning speed within the 2θ range of 10−80°. Scanning electron microscope (SEM) observation was performed using a JEOL JSM-890 scanning electron microscope. TGA patterns were collected on a thermogravimetric analyzer RIGAKU Thermoplus TG8120. The samples were heated in air and the temperature program was 2 K/min.

Results and Discussion

SEM images of activated carbon fibers BW-103, the silica sample calcined in air at 873 K after the treatment in supercritical fluids, and the silica sample treated in oxygen plasma are shown in Figure 2. The cloth shapes are replicated in both of the silica samples (Figure 2b,c). The width of the fibers in the sample treated in oxygen plasma is almost the same as that in the activated carbon BW-103. On the other hand, a little shrinkage

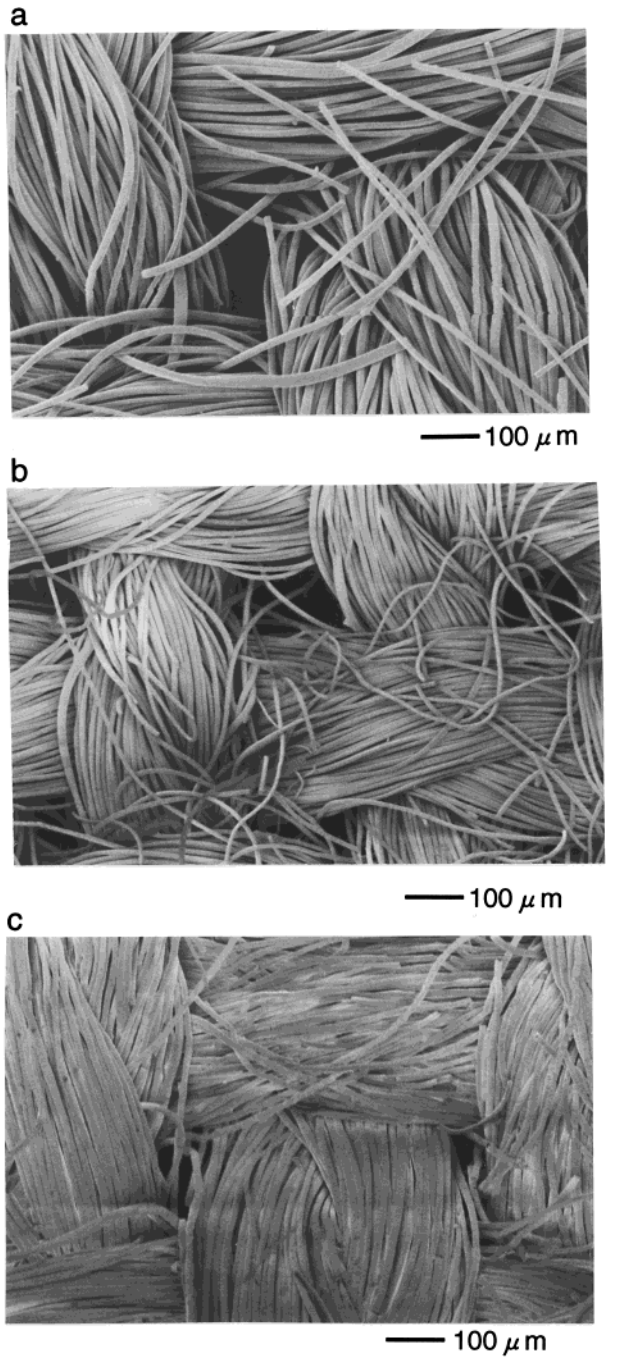

Figure 2. Scanning electron microscopy (SEM) images of (a) activated carbon fibers BW-103, (b) silica sample calcined in air at 873 K after the treatment in supercritical fluids, and (c) the silica sample treated in oxygen plasma after the treatment in supercritical fluids.

can be observed in the calcined sample. As shown in Figure 3, plant structures of the activated carbon from palm nutshells are retained in the silica sample even after the removal of activated carbon templates.

TGA curves of the activated carbon template M30, M30 coated with silica in supercritical CO_2, and sample after removal of M30 by calcination in air from silica-coated M30 using supercritical CO_2 are shown in Figure 4 a−c. Distinct weight losses that would correspond to the removal of activated carbon appeared in Figure 4 a and b in the temperature ranges of 775−893 K and 803−943 K, respectively. Weight losses of activated carbon treated in supercritical CO_2 between 423 K and

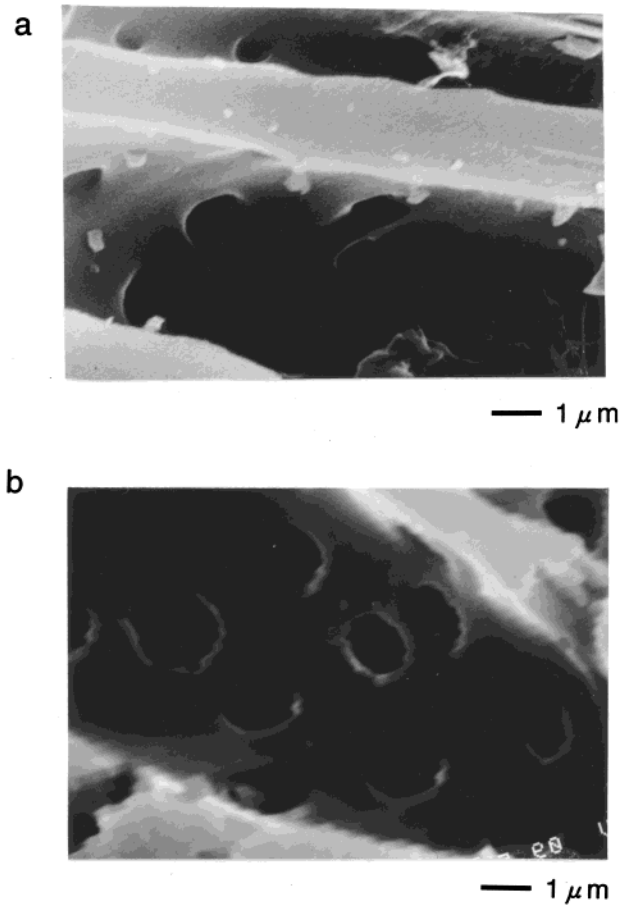

Figure 3. Scanning electron microscopy (SEM) images of (a) activated carbon from palm nutshell GC-2 and (b) silica sample calcined in air at 873 K after the treatment in supercritical.

673 K are 2−5 wt % and are 1−4 wt % greater than that of activated carbon. This may be due to polycondensation of hydrolyzed TEOS. TGA results of silica samples calcined in air or treated with oxygen plasma show that weight losses between 473 K and 1273 K in air flow is less than 3 wt %. This confirms that no activated carbon is present in silica samples.

The nitrogen adsorption−desorption isotherms for activated carbon (A-20, BW103, M30, D7), those coated with silica in supercritical fluids, and samples after the removal of activated carbon by calcination in air or in oxygen plasma are shown in Figures 5−8. Samples prepared by immersion in liquid TEOS are also plotted in Figures 5−8. In Table 1, the pore size, BET surface area, and total pore volume of each activated carbon template and silica sample prepared with supercritical CO_2 or in immersion process are summarized.

As seen in Figure 5, the shape of the isotherm for activated carbon BW-103 shows a typical isotherm for microporous materials. The total pore volume for silica coated activated carbon in supercritical fluids is smaller than that for activated carbon BW-103. This can be attributed to the filling of a part of micropores of activated carbon by silica. When supercritical fluids are used for the silica coating, removal of activated carbon increases the pore volume. The shape of the isotherms for samples after removing activated carbon shows a typical isotherm for mesoporous materials (Figure 5, lines 3 and 4). The pore sizes in the sample treated in oxygen plasma are larger than those of the sample

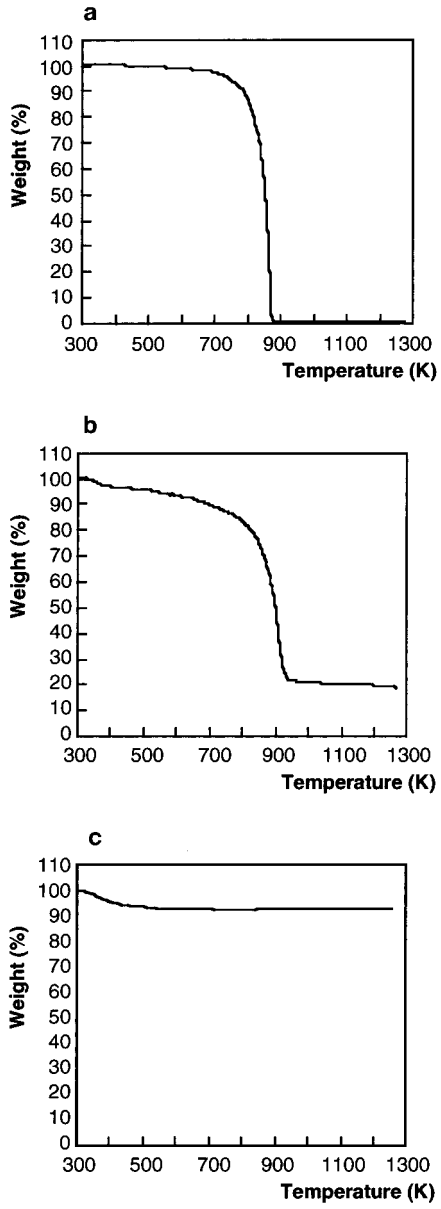

Figure 4. TGA curves for (a) activated carbon template M30, (b) M30 coated with silica in supercritical CO_2, and (c) sample after the removal of M30 by calcination in air from silica coated M30 in supercritical CO_2.

calcined in air. On the other hand, immersion in liquid TEOS decreases the pore volume significantly and silica samples have little surface area even after removing the activated carbon. There is no manifested step corresponding with the existence of micropores or mesopores in the isotherm for the silica sample produced by the immersion process (Figure 5, line 6). It is assumed that silica products cover only entrances of pores of activated carbon, resulting in extensive reduction in pore volume of carbon samples soaked in liquid TEOS. And silica would not be filled deeply into pores. Thus, silica products after the removal of activated carbon have a small amount of pore volume. Similar results as described above are obtained for activated carbon fibers A-20, as illustrated in Figure 6.

There can be seen a slight adsorption−desorption hysteresis in the isotherm for activated carbon powders M30 (Figure 7, line 1). Although total pore volume decreases by the treatment in supercritical fluids (Fig-

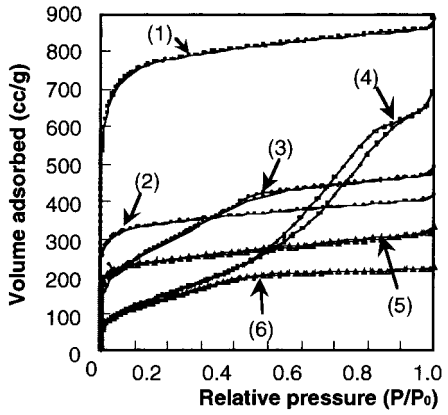

Figure 5. Nitrogen adsorption−desorption isotherms for (1) activated carbon fibers BW-103, (2) BW-103 coated with silica in supercritical CO_2, (3) sample after removal of BW-103 by calcination in air from silica-coated BW-103 in supercritical CO_2, (4) sample after removal of BW-103 by calcination in oxygen plasma from silica-coated BW-103 in supercritical CO_2, (5) BW-103 coated with silica immersed in liquid silica precursor, tetraethlorthosilicate (TEOS), and (6) sample after removal of BW-103 by calcination in air from silica-coated BW-103 in liquid TEOS,

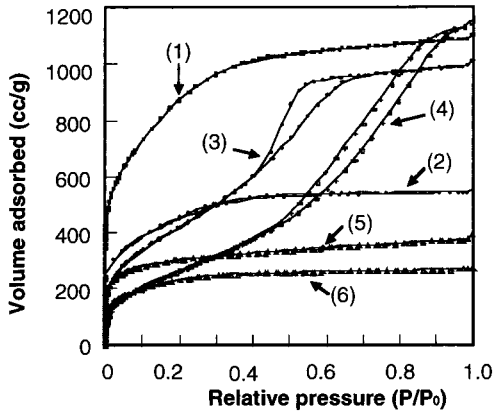

Figure 6. Nitrogen adsorption−desorption isotherms for (1) activated carbon fibers A-20, (2) A-20 coated with silica in supercritical CO_2, (3) sample after removal of A-20 by calcination in air from silica-coated A-20 in supercritical CO_2, (4) sample after removal of A-20 by calcination in oxygen plasma from silica-coated A-20 in supercritical CO_2, (5) A-20 coated with silica immersed in liquid silica precursor, tetraethlorthosilicate (TEOS), and (6) sample after removal of A-20 by calcination in air from silica-coated A-20 in liquid TEOS,

ure 7, line 2), the amount of decrease is not so significant as that for BW-103 or A-20. After removing the activated carbon, hystereses are observed in the isotherms for silica samples and total pore volumes are almost the same as that for the silica-coated sample using supercritical fluids. The hysteresis is also observed for the silica sample prepared by immersion method in liquid TEOS (Figure 7, line 6).

The shape of the isotherm of activated carbon D7 shows the typical isotherm corresponding to the mesoporous materials (Figure 8, line 1) and the BJH pore size is equal to 3.5 nm. The hysteresis also appears in the isotherm for the sample after being coated with silica using supercritical fluids in Figure 8, line 2. The treatment in supercritical fluids decreases pore volume slightly. After activated carbonis removed, mesopores with different sizes appear (Figure 8, line 3 and 4). A hysteresis in the isotherm can be observed even after

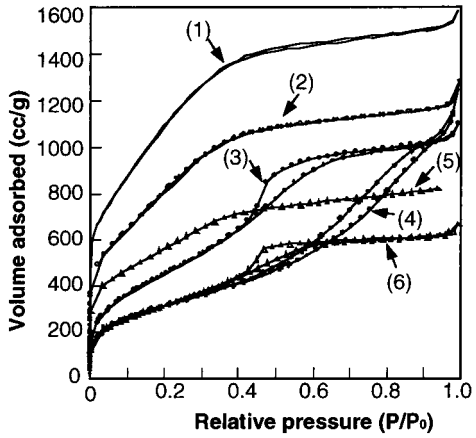

Figure 7. Nitrogen adsorption−desorption isotherms for (1) activated carbon powders M-30, (2) M-30 coated with silica in supercritical CO_2, (3) sample after removal of M-30 by calcination in air from silica-coated M-30 in supercritical CO_2, (4) sample after removal of M-30 by calcination in oxygen plasma from silica-coated M-30 in supercritical CO_2, (5) M-30 coated with silica immersed in liquid silica precursor, tetraethlorthosilicate (TEOS), and (6) sample after removal of M-30 by calcination in air from silica-coated M-30 in liquid TEOS,

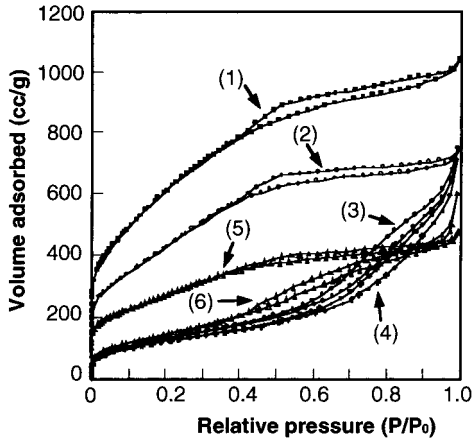

Figure 8. Nitrogen adsorption−desorption isotherms for (1) activated carbon granules D7, (2) D7 coated with silica in supercritical CO_2, (3) sample after removal of D7 by calcination in air from silica-coated D7 in supercritical CO_2, (4) sample after removal of D7 by calcination in oxygen plasma from silica-coated D7 in supercritical CO_2, (5) D7 coated with silica immersed in liquid silica precursor, tetraethlorthosilicate (TEOS), and (6) sample after removal of D7 by calcination in air from silica-coated D7 in liquid TEOS,

the immersion in liquid TEOS (Figure 8, line 5). And mesopores appear in the silica sample prepared by the immersion process (Figure 8, line 6). It would be suggested that some liquid TEOS molecules penetrate into pores of activated carbon D7 during the immersion process and porous structures are roughly replicated in the silica sample after the removal of activated carbon.

The t-plot method was used to calculate micropore volume. The maximum value of micropore volume of the silica samples is 0.339 cm^3/g for the calcined sample at 873 K prepared with activated carbon powders M30. Very few micropores in the samples treated in oxygen plasma were observed. The micropores in the silica samples can be produced as a result of some shrinkage during calcination.

The XRD patterns of activated carbon are given in Figure 9. The sizes of the crystallites in the activated

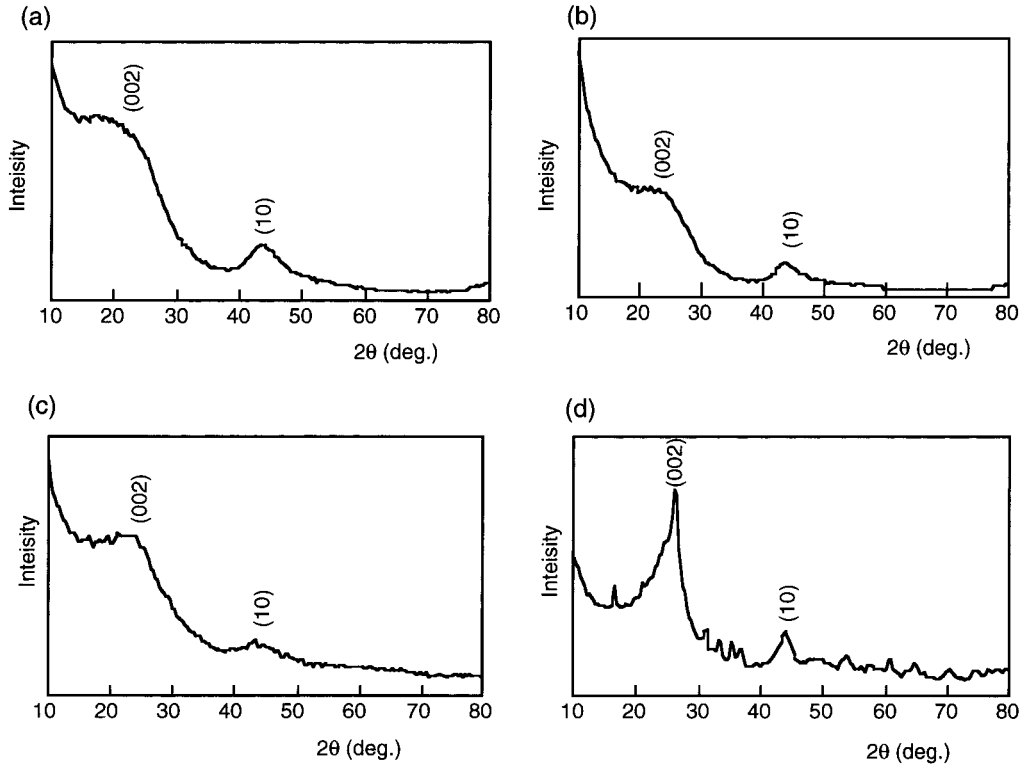

Figure 9. XRD pattern of (a) activated carbon fibers BW-103, (b) activated carbon fibers A-20, (c) activated carbon powders M-30, and (d) activated carbon granules D-7,

Table 1. Characterization of the Porosity of (a) Activated Carbon Template, (b) Activated Carbon Coated with Silica in Supercritical CO_2, (c) Sample after Removal of Activated Carbon by Calcination in Air from Silica-Coated Activated Carbon in Supercritical CO_2, (d) Sample after Removal of Activated Carbon by Calcination in Oxygen Plasma from Silica-Coated Activated Carbon in Supercritical CO_2, (e) Activated Carbon Coated with Silica Immersed in Liquid Silica Precursor, Tetraethlorthosilicate (TEOS), and (f) Sample after Removal of Activated Carbon by Calcination in Air from Silica-Coated Activated Carbon in Liquid TEOS

	activated carbon template	preparation method	method for removal of activated carbon template	pore size (nm)	BET surface area (m^2/g)	total pore volume (cc/g)
a	BW103			1.3	1967	1.37
b	BW103	coat in supercritical CO_2		1.2	683	0.52
c	BW103	coat in supercritical CO_2	calcination in air	3.2	1072	0.77
d	BW103	coat in supercritical CO_2	treatment with oxygen plasma	4.8	608	1.08
e	BW103	immersion in liquid TEOS		1.2	908	0.65
f	BW103	immersion in liquid TEOS	calcination in air	1.4	540	0.35
a	A-20			1.4	1747	1.71
b	A-20	coat in supercritical CO_2		1.4	887	0.86
c	A-20	coat in supercritical CO_2	calcination in air	3.6	984	1.57
d	A-20	coat in supercritical CO_2	treatment with oxygen plasma	4.8	733	1.80
e	A-20	immersion in liquid TEOS		1.2	538	0.61
f	A-20	immersion in liquid TEOS	calcination in air	1.3	444	0.42
a	M30			1.9	3158	2.47
b	M30	coat in supercritical CO_2		1.3	2419	1.99
c	M30	coat in supercritical CO_2	calcination in air	3.7	1377	1.71
d	M30	coat in supercritical CO_2	treatment with oxygen plasma	5.4	889	1.93
e	M30	immersion in liquid TEOS		1.3	1605	1.28
f	M30	immersion in liquid TEOS	calcination in air	3.7	916	1.03
a	D7			3.5	1433	1.61
b	D7	coat in supercritical CO_2		3.3	1022	1.15
c	D7	coat in supercritical CO_2	calcination in air	6.2	480	1.16
d	D7	coat in supercritical CO_2	treatment with oxygen plasma	7.5	447	1.11
e	D7	immersion in liquid TEOS		3.3	987	0.74
f	D7	immersion in liquid TEOS	calcination in air	3.7	539	0.93

carbon fibers BW-103 along with *a* axis L_a and *c* axis L_c are estimated to be 2.2 and 0.9 nm from the half-width of (10) and (002) lines in the XRD pattern (Figure 9a).

The relations between the size of the crystallites along with *a* axis L_a and *c* axis L_c of activated carbon and the average pore sizes of silica samples after the removal of activated carbon by calcination in air or treated in oxygen plasma from silica coated activated carbon in supercritical fluids are compared in Figure 10. The actual sizes of the structural units of activated carbon could not be estimated from only the XRD results, due to disordered structures and functional units. However, the pore size of silica samples after the removal of

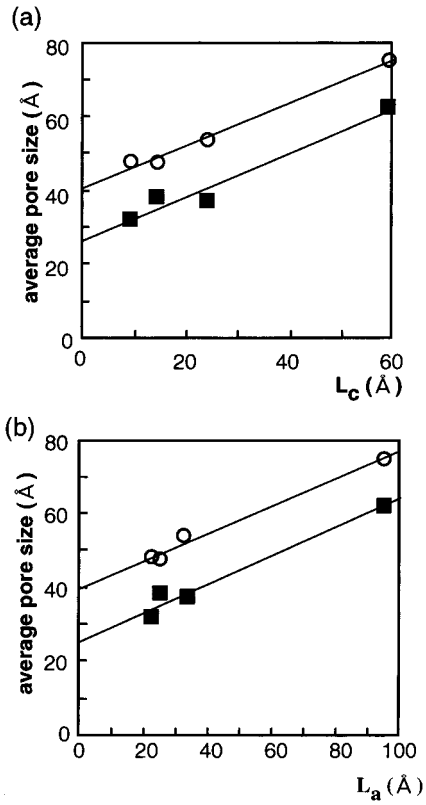

Figure 10. Relations between the size of the crystallites along with *a* axis L_a and *c* axis L_c of activated carbon and the average pore size of silica samples after the removal of activated carbon by calcination in air (closed square) or in oxygen plasma (open circle).

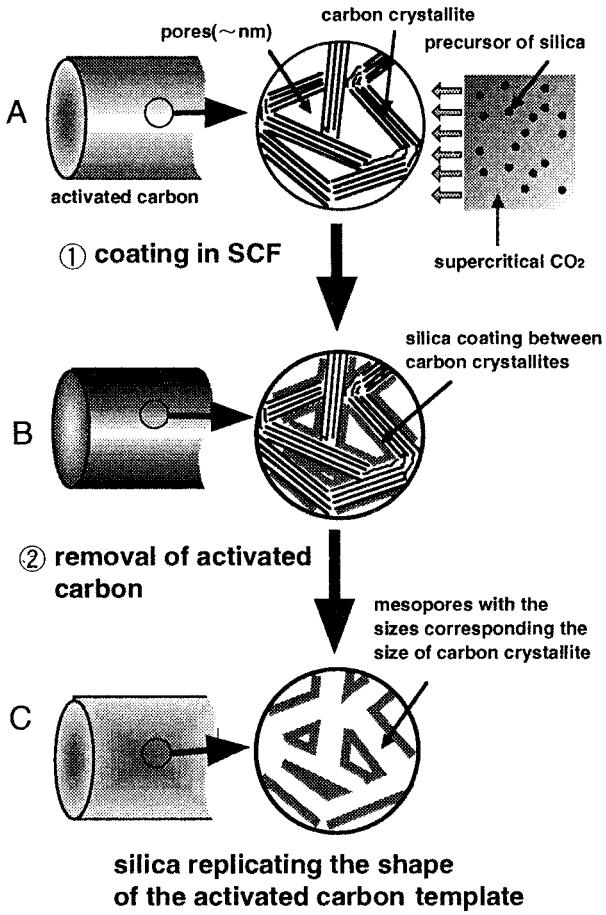

Figure 11. Possible mechanistic pathway for the formation of silica replicas.

activated carbon increases with an increase in crystallite sizes of activated carbon, as shown in Figure 10. And they are in the same order of scale (nanometer). During the treatment in oxygen plasma, only a little rearrangement of silica in the sample would occur because of relatively low temperature of the sample. The maximum temperature during the oxygen plasma treatment is estimated to be 453 K. The porous structures are replicated more faithfully for the samples treated in oxygen plasma than the sample calcined in air. The treatment in air at 873 K yields smaller pores due to some shrinkage.[15]

It is presumed that mesopores with the size corresponding with the size of the graphene layers appear after the removal of activated carbon by calcination in air or by oxygen plasma. Figure 11 shows the possible mechanistic pathway for the formation of silica replicas. The micropores of activated carbon are thought to be spaces between randomly stacked graphene crystallites (Figure 11A). Silica precursor dissolved in supercritical CO_2 is assumed to be carried even into micropores of the activated carbon in the silica coating process. Supercritical CO_2 would act as a carrier, not as a wetting agent that promotes the wettability of the carbon by TEOS. The silica precursors hydrolyze and polymerize to form silica network by the reaction with adsorbed water molecules and hydroxyl units on the surface of activated carbon. The surface of the pores of activated carbon is covered with silica layers (Figure 11B). After the removal of activated carbon, the silica with pores corresponding to the sizes of crystallites of activated carbon remained (Figure 11C).

Conclusions

We have demonstrated the synthesis of microporous and mesoporous silica, replicating both the macroscopic shapes and nanoscale structures of activated carbon molds. The pore size of the silica replicas increases with an increase in carbon crystallite size of the activated carbon as estimated from XRD patterns. Supercritical fluid is shown to be an effective solvent for the reaction (e.g., sol−gel) in nanospaces to produce microporous and mesoporous materials with desired macroscopic shapes. This process can be applied over a range of functional ceramics or metals whose structures are skillfully controlled through the choice of templates.

Acknowledgment. The authors greatly thank Dr. Inagaki, Dr. Setoyama, and Dr. Bhaumik for useful discussions and Mr. Kadoura for taking SEM images.

CM990487E

(15) Iler, R. K., *The Chemistry of Silica*; Wiley: New York, 1979.